

TIN(IV) SCHIFF BASE COMPLEXES: SYNTHESIS, THERMODYNAMIC AND ANTI BACTERIAL INVESTIGATION, EXPERIMENTAL AND THEORETICAL STUDIES

Sheida Esmailzadeh^{1*} and Mohammad Sharif-Mohammadi²

¹Department of Chemistry, Darab branch, Islamic Azad University, Darab, Iran

²Department of Chemistry, Firozabad branch, Islamic Azad University, Firozabad, Iran

(Received December 29, 2017; Revised November 10, 2018; Accepted November 14, 2018)

ABSTRACT. A series of five coordinated diorganotin(IV) unsymmetrical Schiff base complexes have been synthesized. The structure determination and characterization of these complexes were made on the basis of UV-Vis, IR, (¹H and ¹¹⁹Sn) NMR spectroscopy as well as elemental analysis. The binding site of the ligand was identified by IR spectroscopic measurement. Computational analyses at the level of DFT were performed to study its electronic and molecular structures. The molecular geometry, infrared vibrational frequencies, HOMO-LUMO energy gap, dipole moment, Mulliken charges, HF energies were calculated. The theoretical results were consistent with the experimental data reported. The Schiff base ligands and synthesized tin(IV) complexes were screened for their in vitro growth inhibiting activity against different strains of bacteria. Results indicated that the complexes exhibited good antibacterial activities than the ligands. Also the thermodynamic formation constants of the Schiff bases as donors with Me₂SnCl₂ as an acceptor were measured using UV-Vis spectrophotometric titration for 1:1 complex formation at constant ionic strength (I = 0.1 M NaClO₄) and at 25 °C.

KEY WORDS: Tin(IV) complexes, Thermodynamic parameter, Biological activity, Computational analyses

INTRODUCTION

The discovery of several new organotin species and new applications has led to a renewed interest in organotin complexes. A large number of organotin compound are used in several areas such as pharmaceuticals, pesticides, stabilizers, fire retardants, miticides, molluscicides, marine antifouling paints, surface disinfectants and wood preservatives and many more [1-4]. On the other hand, Schiff base ligands received instant and enduring popularity because they have played a seminal role in the development of modern coordination chemistry, as well as they can also be found at key points in the development of inorganic chemistry, catalysis, pigment and dyes, medicinal imaging, optical materials and thin films [5-8]. Schiff base ligands containing hetero atoms such as N, O, and S show a broad biological activity and are of special interest because of their variety of ways in which they are interacted to metal ions. Schiff base in neutral and deprotonated forms react with organotin(IV) halides and the complexes extensively studied because they have some characteristics properties like manifestations of novel structures, thermal stability, high synthesis flexibility, medicinal utility, industrial applications and relevant biological properties [9-12]. In addition to their special antimicrobial activities, organotin(IV) compound with Schiff bases present an interesting variety of structural possibilities, so that a remarkable diversity in structure may be observed even when only a small change in the chemistry occurs [13].

The present study will entail a description of synthesis and characterization of some tin(IV) complexes with Schiff bases containing sulfur, nitrogen and oxygen atoms, and illustration of the geometrical structure by using spectral analysis. By comparing the spectral and thermodynamic properties of Schiff base ligands and their complexes, we aimed to investigate the effects of different electronic and steric behaviors. Moreover, the density functional theory computational calculations were done for tin(IV) Schiff base complexes for comparing with experimental results. Also, the present work involves antibacterial activities against gram-positive and gram-negative bacterial for the Schiff base ligand and their complexes.

*Corresponding author. E-mail: esmailzadehsheida@yahoo.com

This work is licensed under the Creative Commons Attribution 4.0 International License

EXPERIMENTAL

Materials and physical measurements

All chemicals and reagents were commercially available and were grade quality. All the reagents were used as received. The infrared spectra of the solid compounds were recorded on a Shimadzu FTIR 8300 spectrophotometer in the range 4000-200 cm^{-1} as KBr discs. The melting points were determined in open capillaries with electronic melting point apparatus. C, H, N, S analyses were carried on a Termo Fininngan-Flash-1200. The ^1H and ^{119}Sn NMR spectral data were obtained on Bruker Avance DPZ 500 MHz spectrometer using TMS and SnMe_4 as references and chemical shift are expressed in ppm. The conductivity were performed using Jenway 4310 conductivity meter and a diptype cell with a platinized electrode in DMF having 10^{-3} M solutions of the metal complexes at room temperature. UV-Vis spectra were recorded in DFT with T80 UV-Vis spectrophotometers.

Preparation of ligands and corresponding complexes

The unsymmetrical Schiff base ligands was synthesized by stirring at room temperature a 1:1 molar ratio mixture of methyl-2-(1-methyl-2'-amino-ethane)amino-1-cyclopentenedithiocarboxylate [HcdMeen] and the substituted salicylaldehyde in methanolic solution following a reported method [14-16]. The resultant yellow powder was recrystallized from methanol/chloroform 2:1 (v:v). To a stirred solution of methyl-2-[[1-methyl-2-(2-hydroxy-5-methoxyphenyl)methylidynenitrilo]ethyl]amino-1-cyclopentenedithiocarboxylate [$\text{H}_2\text{cd5OMesalMeen}$], methyl-2-[[1-methyl-2-(2-hydroxyphenyl)methylidynenitrilo]ethyl]-amino-1-cyclopentenedithiocarboxylate, [$\text{H}_2\text{cdsalMeen}$], methyl-2-[[1-methyl-2-(2-hydroxy-5-bromophenyl)methylidynenitrilo]ethyl]amino-1-cyclopentenedithiocarboxylate, [$\text{H}_2\text{cd5-BrsalMeen}$], methyl-2-[[1-methyl-2-(2-hydroxy-5-chlorophenyl)methylidynenitrilo]ethyl]-amino-1-cyclopentene-dithiocarboxylate, and [$\text{H}_2\text{cd5-ClsalMeen}$] methyl-2-[[1-methyl-2-(2-hydroxy-5-nitrophenyl)methylidynenitrilo]ethyl]amino-1-cyclopentenedithiocarboxylate, [$\text{H}_2\text{cd5-NO}_2\text{salMeen}$] (1 mmol) in 15 mL of chloroform/methanol 2:1(v:v), a solution of Me_2SnCl_2 (1 mmol) in 15 mL of methanol was added slowly at r.t. The mixture was then stirred for 4-6 h. During this period, the yellow solid precipitate formed was filtered and washed with petroleum ether (Figure 1).

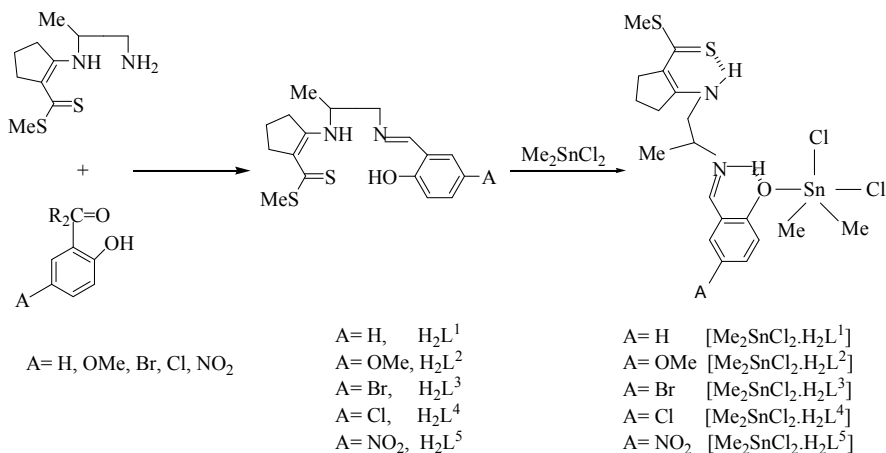


Figure 1. Schematic representation of the Sn(IV) complexes.

Thermodynamic studies of complex formation

The formation constants, K_f , of the Sn(IV) complexes were determined by spectrophotometric titration of the ligands H₂cdXsalMeen with various concentration of the solution of dimethyltin(IV)dichloride at constant ionic strength (0.1 M NaClO₄) at 25 °C. The interaction of NaClO₄ with the ligands was negligible. In a typical measurement, 2.5 mL of the ligand solution (10⁻⁵ M) in DMF was transferred into the thermostated cell compartment of UV-Visible instrument, and was titrated by the dimethyltin(IV)dichloride solution (10⁻⁵-10⁻⁴ M) in DMF. The titration was performed by adding aliquots of the tin ion with a Hamilton µL syringe to the ligand. The UV-Vis spectra were recorded in the range 290-600 nm about 5 min after each addition. The formed product showed different absorption from the free ligand, while the metal ion solution shows no absorption at those wavelengths. As an example, the variation of the electronic spectra for [H₂L⁵] titrated with various concentration of dimethyltin(IV)dichloride at 25 °C in DMF. The same procedure was followed for other systems. The electronic spectra of the formed complexes at the end of titration were the same as the electronic spectra of the separately synthesized complexes.

Determination of bacteriological activity

Bioactivities were investigated using agar-well diffusion method [17]. The synthesized Schiff base ligands and their tin(IV) complexes were screened for their biological activities by using two bacteria namely *Staphylococcus aureus* and *Escherichia coli* by the reported method. The bacteria were subcultured in agar medium. Recommended concentration (100 µL) of the test sample 1 mg/mL in DMSO was introduced in the respective wells. The Petri dishes were incubated immediately for 24 hours at 37 °C. Activity was determined by measuring the diameter of the zone showing complete inhibition (mm). Growth inhibition was compared with standard drugs. In order to clarify the role of DMSO on the biological screening, separate studies were carried out with solvent DMSO only and it showed no activity against any microbial strains.

Theoretical methods

The quantum chemical calculations were performed using Gaussian 03 package [18]. The local minimum energy, Mulliken charges, dipole moment, HOMO-LUMO energy and its band gap of the optimized structures for Sn(IV) complexes was computed at Becke three parameter hybrid function (B3LYP) using LANL2DZ and 6-311G** basis sets for all atoms including tin [19]. By the use of LANL2DZ basis set, computational time and convergence difficulties were considerably reduced. LANL2DZ basis set uses pseudopotential, the results are very close to the experimental data. This does not necessarily substantiate preference of LANL2DZ basis set over 6-311G**. Many descriptors were used to recognize and correlate some physical and chemical properties. The calculated vibrational spectra of the optimized complexes were assigned based on vibrational mode analysis with the aid of the DFT method.

RESULTS AND DISCUSSION

Elemental analysis

The stoichiometry of the tin(IV) complexes were confirmed by their elemental analysis. Experimental and calculated elemental compositions of the complexes are given in Table 1. The analytical data are in good agreement with the proposed structures of the complexes (Figure 1). The metal/ligand ratio was found to be 1:1 has been arrived at by estimating the carbon, hydrogen, nitrogen and sulfur contents of the complexes. Solutions of these complexes no react with silver nitrate indicating the existence of chloride in inside coordination sphere of the tin ion.

Molar conductance

The tin(IV) complexes under investigation are quite stable at ambient temperature. They are sparingly soluble in donor solvents such as DMF and DMSO. The molar conductance of these complexes (Table 1) indicating that it is essentially a non-electrolyte in this solvent [20]. The very low conductance for these complexes is strong evidence that the Schiff base is coordinated to the tin atom as an unnegatively charged ligand and that the two chloro ligands are also coordinated to the tin ion.

Infrared spectra

The IR spectra give enough information to elucidate the nature of bonding of the ligand to the metal ions. The IR spectra of free Schiff base were compared with the spectra of the tin(IV) complexes in order to study the binding mode of the Schiff base to Sn(IV) ion in the new complexes. In Table 2 the main infrared bands and their assignments are shown. In this spectra of free ligand and new complexes no band is observed in the region 3500-3600 cm^{-1} attributable to the stretching vibration of the free phenolic OH group indicating that the ring formed by the intramolecular hydrogen bond in the ligand which, is retained in complexes. Weak broad absorption bands appearing in the range of 2800-2900 cm^{-1} for the free Schiff base ligands are assigned to $\nu(\text{O-H})$ and $\nu(\text{N-H})$ overlapping with the $\nu(\text{C-H})$ [16]. These bands are observed to shift slightly to higher frequency due to the coordination of phenolic oxygen atom with tin and changes in hydrogen bonding [21]. The strong bands at 1622-1649 cm^{-1} , which can be attributed to $\nu(\text{C=N})$ stretching frequency on Schiff base ligands [16]. This band showed a major shift to higher frequency (1638-1659 cm^{-1}) is suggesting the complex formation and the proton transfer from phenolic oxygen atom to the imine nitrogen atom [22]. In the spectra of tin(IV) complexes a sharp peak at 1558-1567 cm^{-1} due to the $\nu(\text{C=O})$ providing evidence of participation of the phenolic oxygen in the tin-ligand bonding [23]. The aromatic $\nu(\text{C=C})$ stretching frequency occurs at 1479-1497 cm^{-1} [24]. The characteristic sulfur vibration of $\nu(\text{C-S})$ appearing at 763-798 cm^{-1} [16].

Table 1. Physical properties and analytical data of the synthesized tin(IV) complexes.

Complexes	Empirical formula	Formula weight	Yield (%)	$\Lambda_M(\Omega^{-1} \text{cm}^2 \text{mol}^{-1})$	m.p. ($^{\circ}\text{C}$)	Anal. found (calc.) (%)			
						C	H	N	S
$[\text{Me}_2\text{SnCl}_2 \cdot \text{H}_2\text{L}^1]$	$\text{C}_{19}\text{H}_{28}\text{N}_2\text{Cl}_2\text{O}_2\text{S}_2\text{Sn}$	554.15	49	20	170	41.07(41.18)	5.21(5.09)	5.11(5.06)	11.64(11.57)
$[\text{Me}_2\text{SnCl}_2 \cdot \text{H}_2\text{L}^2]$	$\text{C}_{20}\text{H}_{30}\text{N}_2\text{Cl}_2\text{O}_2\text{S}_2\text{Sn}$	584.18	53	20	173	41.22(41.12)	5.46(5.18)	4.66(4.80)	10.75(10.98)
$[\text{Me}_2\text{SnCl}_2 \cdot \text{H}_2\text{L}^3]$	$\text{C}_{19}\text{H}_{27}\text{N}_2\text{Cl}_2\text{O}_2\text{S}_2\text{BrSn}$	633.05	49	15	161	35.93(36.05)	4.21(4.30)	4.697(4.43)	10.36(10.13)
$[\text{Me}_2\text{SnCl}_2 \cdot \text{H}_2\text{L}^4]$	$\text{C}_{19}\text{H}_{27}\text{N}_2\text{Cl}_2\text{O}_2\text{S}_2\text{Sn}$	588.60	51	17	168	39.13(38.77)	4.54(4.62)	5.05(4.76)	11.03(10.89)
$[\text{Me}_2\text{SnCl}_2 \cdot \text{H}_2\text{L}^5]$	$\text{C}_{19}\text{H}_{27}\text{N}_3\text{Cl}_2\text{O}_3\text{S}_2\text{Sn}$	599.15	47	21	157	38.39(38.09)	4.68(4.54)	7.15(7.01)	10.51(10.70)

Table 2. Selected experimental and theoretical IR frequencies (cm^{-1}) of Sn(IV) Schiff base complexes.

	Complexes	$\nu(\text{Sn-O})$	$\nu(\text{C-S})$	$\nu(\text{C=C})$	$\nu(\text{C=O})$	$\nu(\text{C=N})$	$\nu(\text{C-H})$
		m	br, m	s	s	vs	m
Experimental frequencies	$[\text{Me}_2\text{SnCl}_2 \cdot \text{H}_2\text{L}^1]$	591	763	1480	1563	1638	2867
	$[\text{Me}_2\text{SnCl}_2 \cdot \text{H}_2\text{L}^2]$	584	790	1485	1558	1659	2925
	$[\text{Me}_2\text{SnCl}_2 \cdot \text{H}_2\text{L}^3]$	587	766	1475	1567	1638	2917
	$[\text{Me}_2\text{SnCl}_2 \cdot \text{H}_2\text{L}^4]$	587	798	1477	1565	1641	2971
	$[\text{Me}_2\text{SnCl}_2 \cdot \text{H}_2\text{L}^5]$	590	774	1473	1559	1657	2944
Calculated frequencies	$[\text{Me}_2\text{SnCl}_2 \cdot \text{H}_2\text{L}^1]$	590	767	1495, 1475	1567	1642	2872
	$[\text{Me}_2\text{SnCl}_2 \cdot \text{H}_2\text{L}^2]$	589	785	1750, 1560, 1477	1561	1663	2927
	$[\text{Me}_2\text{SnCl}_2 \cdot \text{H}_2\text{L}^3]$	585	769	1492, 1483, 1476	1573	1645	1921
	$[\text{Me}_2\text{SnCl}_2 \cdot \text{H}_2\text{L}^4]$	586	802	1492, 1481, 1476	1562	1645	2973
	$[\text{Me}_2\text{SnCl}_2 \cdot \text{H}_2\text{L}^5]$	593	779	1490, 1470, 1474	1565	1661	2949

vs: very strong; s: strong; m: medium; w: weak; br: broad.

New bands in the range of 580-590 cm^{-1} which are not present in the free Schiff base are due to $\nu(\text{Sn-O})$ vibration [25] and the appearance of the vibrations support the involvement of the oxygen atoms of phenolic group complexation with the tin ion under investigations. Two sharp peaks at around 1300 and 1550 cm^{-1} are typical of nitro group in $[\text{Me}_2\text{SnCl}_2 \cdot \text{H}_2\text{cd}5\text{NO}_2\text{salMeen}]$ [16].

^1H and ^{119}Sn NMR spectra

The NMR spectrum is recorded to confirm the binding sites during the complexation. The NMR data are given in Table 3. The chemical shift observed for the $-\text{OH}$ and $-\text{NH}$ protons in free Schiff base ligands (δ 12.45-14.06 ppm) and (δ 12.30-12.38 ppm) was observed in all complexes. The deshielding of this group and shifted down field in complexes may be due to bonding of the oxygen to the tin(IV) ion which lead to decrease of the density of electrons on the hydroxyl group. The same results were confirmed by the IR spectroscopy. The signal at 8-9 ppm were assigned to imine proton ($\text{HC}=\text{N}$) is not flanked by satellites, this is an indicating that the N atom is not coordinated to tin(IV) [26]. The lack of down field shift in the position of the signal attributable to S-CH_3 (δ 2.55-2.57 ppm in free ligand) indicates no participation of the $-\text{C}=\text{S}$ group in binding [27]. The ligand shows multiplet signal in the region δ 6.83-8.23 ppm for the aromatic protons and these values are remains almost same position in the spectra of Sn(IV) complexes. ^1H NMR spectra of Schiff base ligands and their complexes show one peak at chemical shift ca. 1.39-1.41, this singlet peak with three proton integration has been assigned to the methyl group on diamine bridge. The high field regions in the spectra of dimethyl tin show signal at 1.15 ppm for all complexes and these are due to the methyl groups in the organotin fragment. These signals have satellites due to coupling with tin (2J $^{119}\text{Sn-H}$ 71.0 and 77.1 Hz). The data describe above are all consistent with those observed for the other five coordinated diorganotin complexes containing Schiff base ligands [28].

The value of chemical shift ^{119}Sn spectra expresses the coordination number of the nucleus in the related metal complexes. In general, ^{119}Sn chemical shifts move to lower frequency with increasing coordination number of the nuclei. In order to confirm the geometry of the complexes, ^{119}Sn NMR spectra were recorded. The spectra in each complex show only a sharp singlet, indicating the formation of a single species. The ^{119}Sn NMR spectra of all titled complexes $[\text{Me}_2\text{SnCl}_2 \cdot \text{H}_2\text{L}^{1-3}]$ give sharp signals at -166.65, -163.55, -161.43, -161.76, -168.93 ppm, respectively, which is indicative of five coordinated environment around the tin atom. Thus on the basis of the above evidences it is suggested that the geometry of the resulting tin complexes be characterized as trigonal bipyramidal [21, 29, 30]. The proposed structures of newly synthesized complexes are shown in Figure 1.

Table 3. ^1H and ^{119}Sn NMR spectral data of prepared complexes (δ /ppm).

	H_2L^1	$[\text{Me}_2\text{SnCl}_2 \cdot \text{H}_2\text{L}^1]$	H_2L^2	$[\text{Me}_2\text{SnCl}_2 \cdot \text{H}_2\text{L}^2]$	H_2L^3	$[\text{Me}_2\text{SnCl}_2 \cdot \text{H}_2\text{L}^3]$
^1H NMR data	1.41 (d, 3H, Me), 2.56 (s, 3H, SCH_3), 23.54-3.59 (m, 3H, H^{ar}), 6.88 (dd, 1H, H^5), 6.96 (d, 1H, H^3), 7.22-7.31 (m, 2H, $\text{H}^{4,6}$), 8.38 (s, 1H, $\text{CH}=\text{N}$), 12.38 (br, 1H, NH), 12.93 (br, 1H, OH);	1.15 (s, 6H, Sn-Me), 1.41 (3H, d, Me), 2.56 (3H, s, SCH_3), 2.61 (3H, H^{ar}), 3.54-3.59 (3H, m, H^{ar}), 6.87 (1H, dd, H^5), 6.95 (1H, d, H^3), 7.23-7.33 (2H, m, $\text{H}^{4,6}$), 8.38 (1H, s, $\text{CH}=\text{N}$), 12.41 (1H, br, NH), 13.05 (1H, br, OH)	1.39 (d, 3H, Me), 2.56 (s, 3H, SCH_3), 3.52-3.55 (m, 3H, H^{ar}), 3.77 (s, 3H, OCH_3), 6.73 (s, 1H, H^9), 6.86 (d, 1H, H^4), 7.24 (d, 1H, H^3), 8.28 (s, 1H, $\text{CH}=\text{N}$), 12.37 (br, 1H, NH), 12.45 (br, 1H, OH);	1.15 (s, 6H, Sn-Me), 1.39 (3H, d, Me), 2.56 (3H, s, SCH_3), 3.52-3.55 (3H, m, H^{ar}), 3.77 (3H, s, OCH_3), 6.77 (1H, s, H^6), 6.83 (1H, H^6), 7.21 (1H, d, H^4), 8.11 (1H, s, $\text{CH}=\text{N}$), 12.42 (1H, br, NH), 12.55 (1H, br, OH)	1.39 (d, 3H, Me), 2.57 (s, 3H, SCH_3), 3.49-3.88 (m, 3H, H^{ar}), 6.83 (d, 1H, H^5), 7.34 (s, 1H, H^3), 7.40 (d, 1H, H^4), 8.27 (s, 1H, $\text{CH}=\text{N}$), 12.33 (br, 1H, NH), 12.93 (br, 1H, OH)	1.15 (s, 6H, Sn-Me), 1.39 (3H, d, Me), 2.56 (3H, s, SCH_3), 3.50-3.86 (3H, m, H^{ar}), 6.85 (1H, d, H^5), 7.18-7.27 (1H, m, H^3), 7.40 (d, $\text{H}^{4,6}$), 8.32 (1H, s, $\text{CH}=\text{N}$), 12.39 (1H, br, NH), 12.97 (1H, br, OH)
^{119}Sn NMR data		-166.65		-163.55		-161.43

Table 3. Continues

	H ₂ L ⁴	[Me ₂ SnCl ₂ .H ₂ L ⁴]	H ₂ L ⁵	[Me ₂ SnCl ₂ .H ₂ L ⁵]
¹ H NMR data	1.39 (d, 3H, Me), 2.56 (s, 3H, SCH ₃), 3.50-3.86 (m, 3H, H ^m), 6.88 (d, 1H, H ³), 7.20-7.28 (m, 1H, H ^{4,6}), 8.32 (s, 1H, CH=N), 12.32 (br, 1H, NH), 12.91 (br, 1H, OH)	1.15 (s, 6H, Sn-Me), 1.39 (3H, d, Me), 2.57 (3H, s, SCH ₃), 3.49-3.88 (3H, m, H ^m), 6.80 (1H, d, H ³), 7.32 (1H, s, H ⁶), 7.38 (1H, d, H ⁴), 8.27 (1H, s, CH=N), 12.38 (1H, br, NH), 13.01 (1H, br, OH)	1.43 (d, 3H, Me), 2.55 (s, 3H, SCH ₃), 3.61-3.66 (m, 3H, H ^m), 6.99 (d, 1H, H ³), 8.20-8.23 (m, 2H, H ^{4,6}), 8.46 (s, 1H, CH=N), 12.30 (br, 1H, NH), 14.06 (br, 1H, OH)	1.15 (s, 6H, Sn-Me), 1.43 (3H, d, Me), 2.55 (3H, s, SCH ₃), 3.61-3.66 (3H, m, H ^m), 6.97 (1H, d, H ³), 8.18-8.20 (2H, m, H ^{4,6}), 8.46 (1H, s, CH=N), 12.37 (1H, br, NH), 14.14 (1H, br, OH);
¹¹⁹ Sn NMR data		-161.76		-168.93

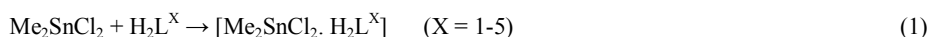
Therefore, it is clear from these results that the data obtained from the elemental analysis, IR and NMR spectral measurements are in agreement with each other.

UV-Vis absorption spectra

The electronic absorption spectra of all the synthesized ligands and their complexes at very low concentrations ($\sim 10^{-4}$ M range) are recorded in DMF solution. The ligands exhibit the band at 312-314 and 395-398 nm can be assigned to intra ligand to $\pi \rightarrow \pi^*$ and $n \rightarrow \pi^*$ transition [16]. Complex formation with dimethyltin(IV)dichloride results changes of the spectra took place in the UV-Vis region (250-600 nm) of $\pi \rightarrow \pi^*$ and $n \rightarrow \pi^*$ absorption band upon this interaction. After coordination of Schiff base to Me₂SnCl₂, the original peaks of the Schiff base ligands changed and have a red shift. A new peak is appeared in 460-470 nm regions. It seems that this is an LMCT from n_o to Sn(IV) via coordination of Schiff base ligand to dimethyltindichloride [31].

The formation constants and the thermodynamic free energy interpretations

To interpret the steric and the electronic parameters of the ligands on the formation constants and the thermodynamic free energy of the complexation, the interaction between five ligands (H₂L¹⁻⁵) and dimethyltindichloride (Me₂SnCl₂) was carried out by UV-Vis absorption spectroscopy through titration of the ligands with various concentrations of the Sn(IV) ion at 25 °C. The complex formation constants, K_f, were calculated using SQUAD computer program [32], designed to calculate the best values for the formation constants of the proposed equation model (Eq. (1)) by employing a non-linear, least-squares approach.



Also, the free energy change, ΔG° , of the complexes were determined by $\Delta G^\circ = -RT \ln K_f$, at 25 °C (Table 4). As the results show, In the *para* substituted Schiff base ligands, the formation constants varies as can be expected according to the electronic effects of the substituents at position 5. Thus, the formation constants decreases according to the sequence OMe > H > Br > Cl > NO₂. This is somewhat in agreement with decreasing electron releasing character of the substituents in the same direction, which result in a decrease in basicity of the phenolic oxygen groups of the ligand, and consequently decreased tendency toward complex formation. The withdrawing functional groups make the Schiff base as a poor donor ligand and decrease the formation constants while the electron donor group increasing the formation constants because they leads to increase the donor ability of Schiff base ligands. Therefore, the ligands having NO₂ group, [H₂L⁵], have the smallest formation constants while the ligands with OMe group, [H₂L²], have the highest because OMe is a donating group. Therefore, in the stabilization of the

complexes, the donation power of the Schiff base is important, and hence their formation constants, K_f , with donation are higher.

Table 4. The formation constants and the free energy values of tin(IV) complexes at 25 °C in DMF.

Complexes	$\log K_f$	ΔG° (kJmol ⁻¹)
[Me ₂ SnCl ₂ .H ₂ L ¹]	7.47(0.11) ^a	-42.54(0.27)
[Me ₂ SnCl ₂ .H ₂ L ²]	7.63(0.13)	-43.51(0.32)
[Me ₂ SnCl ₂ .H ₂ L ³]	7.21(0.09)	-41.12(0.22)
[Me ₂ SnCl ₂ .H ₂ L ⁴]	7.17(0.12)	-40.89(0.29)
[Me ₂ SnCl ₂ .H ₂ L ⁵]	6.93(0.06)	-39.52(0.14)

^aThe numbers in parentheses are the standard deviations.

Antibacterial activity results

The free Schiff base ligands and their corresponding tin(IV) complexes were tasted against the selected bacteria *E.coli* (G-) and *S. aureus* (G+). The measured zones of inhibition against of various microorganisms are summarized in Table 5. All the tested compounds showed good biological activity against microorganism. It is found that the complexes have higher antimicrobial activity than the free ligands. This can be explained on the Tweedy's chelation theory [33]. The lipid membrane that surrounds the cell favors the passage of only lipid soluble materials due to which lipophilicity is an important factor which controls the antimicrobial activity. On chelation, the polarity of the metal ion will be reduced to a greater extent due to the overlap of the ligand orbital and partial sharing of the positive charge of the metal ion with the donor groups. Further, it increases the delocalization of p-electron over the whole chelate ring and hence enhances the liposolubility of the complexes. This increased liposolubility enhances the penetration of the complexes into the lipid membrane, the lipophilic group to derive the compound through the semipermeable of the cell, and blocks the metal binding sites in the enzymes of the microorganism.

Table 5. The Growth inhibition zone of the Schiff base ligands and their Sn(IV) complexes.

Bacteria	Standard (Streptomycin)	Zone of inhibition in nm (25 µg/disc)									
		H ₂ L ¹	[Me ₂ SnCl ₂ .H ₂ L ¹]	H ₂ L ²	[Me ₂ SnCl ₂ .H ₂ L ²]	H ₂ L ³	[Me ₂ SnCl ₂ .H ₂ L ³]	H ₂ L ⁴	[Me ₂ SnCl ₂ .H ₂ L ⁴]	H ₂ L ⁵	[Me ₂ SnCl ₂ .H ₂ L ⁵]
<i>S. Aureus</i>	22	11	17	13	19	10	15	12	16	11	16
<i>E. Coli</i>	24	10	15	12	16	8	18	10	19	12	15

Computational details

The molecular properties of the complex structures under investigation were determined by density functional theory (DFT). The important structural analysis referring to bonding distances, bonding angles and dihedral angles parameters for all optimized structures of Sn(IV) complexes in the ground state configuration are gathered in Table 6. The fully optimized molecular structures of the tin(IV) complexes with atomic numbering are shown in Figure 2.

The structure shows that the complex is monomer in which the tin atom adopts a five-coordinate geometry being ligated to two chloride ions, two carbon atoms of methyl group and O atom of the H₂L¹⁻⁵ ligands. The Schiff base is coordinated to the tin atom as a neutral chelating agent in it is without deprotonated phenolic form via the hydroxyl oxygen atom. The two Sn-Cl42 and Sn-Cl43 bond lengths are similar and the calculated value is longer than Sn-C44, Sn-C45 and Sn-O38 (0.25-0.63 Å).

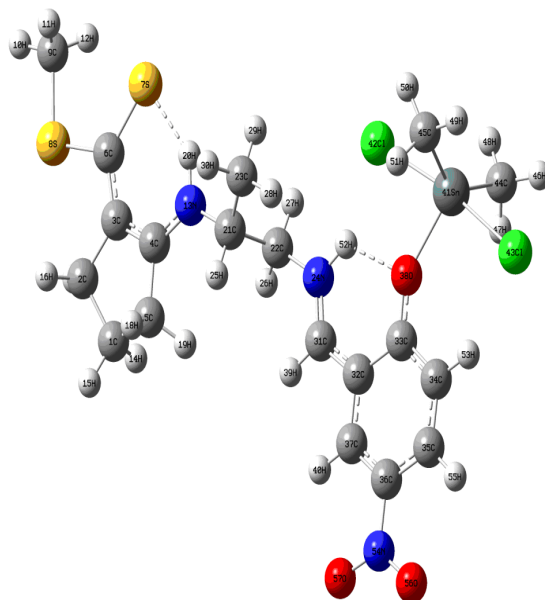


Figure 2. The optimized structures of the $[\text{SnMe}_2\text{Cl}_2 \cdot \text{H}_2\text{L}]^5$.

Table 6. Part of the data of bond distances (Å), bond angles and dihedral angles (°) obtained through B3LYP/LANL2DZ level of theory, labels for atoms can be found in Figure 2.

Bond length (Å)	$[\text{Me}_2\text{SnCl}_2 \cdot \text{H}_2\text{L}]^1$	$[\text{Me}_2\text{SnCl}_2 \cdot \text{H}_2\text{L}]^2$	$[\text{Me}_2\text{SnCl}_2 \cdot \text{H}_2\text{L}]^3$	$[\text{Me}_2\text{SnCl}_2 \cdot \text{H}_2\text{L}]^4$	$[\text{Me}_2\text{SnCl}_2 \cdot \text{H}_2\text{L}]^5$
Sn-Cl43	2.652	2.656	2.649	2.652	2.643
Sn-Cl42	2.673	2.669	2.668	2.664	2.665
Sn-O38	2.039	2.035	2.046	2.046	2.063
Sn-C44	2.120	2.120	2.119	2.119	2.118
Sn-C45	2.119	2.119	2.119	2.119	2.118
O38-H52	2.047	2.019	2.050	2.046	2.077
S7-H20	2.233	2.233	2.231	2.230	2.226
N24-C31	1.319	1.434	1.318	1.318	1.315
N13-C4	1.357	1.335	1.358	1.357	1.359
Bond angle (°)					
Cl42-Sn-Cl43	179.04	179.73	179.88	179.97	179.81
O38-Sn-Cl43	90.97	90.75	90.15	90.26	90.57
O38-Sn-Cl42	80.07	90.99	89.74	89.25	89.25
Cl43-Sn-C44	92.70	90.86	93.13	93.25	93.52
Cl42-Sn-C45	89.46	89.06	89.12	89.75	89.20
O38-Sn-C45	119.87	120.04	120.11	120.13	120.15
O38-Sn-C44	119.98	120.11	120.08	120.12	120.23
Dihedral angle (°)					
O38-C33-C32-C31	-0.06	-0.11	-0.17	0.41	-0.11
N13-C4-C3-C6	0.13	-0.03	0.04	0.28	0.11

The DFT estimated bond lengths are generally overestimated. The coordination geometry can be viewed as a trigonal bipyramidal with the two C atoms and O atom remains in the equatorial position and two Cl atoms in the axial position. In view of the bond angle, Cl42-Sn-Cl43 angles make approximately a 180° angle and the calculated C45-Sn-C44,

C45-Sn-O38 and C44-Sn-O38 angles are 120° respectively (Table 6). On the basis of the results the *tbp* structure was confirmed.

The Sn(IV)-Schiff base ligand interaction is not lead to twisting of the ligand compared to the free ligand. In the optimized structure of the complexes cyclopentene and benzene ring are in the same plane. Their planes make approximately a 2° dihedral angle to each other. The calculated O38-C33-C32-C31 and N13-C4-C3-C6 dihedral angles are near to each other. These molecules are not twisted, so that the 5-X substituents group (5-OMe, 5-H, 5-Br, 5-Cl, 5-NO₂) is in opposite orientation. The aromatic rings are essentially planar, where the bond lengths of C=C (142.9-143.7 Å) are in the expected range [34]. The two O38-H52 and S7-H20 asymmetrical intramolecular hydrogen bonds with distances 2.046-2.077 and 2.226-2.233 Å [35]. However, the two C-N bond lengths differ significantly of the two types of C-N bonds, the bond length for the imine nitrogen (N24=C31) is 0.038-0.044 Å shorter than that for primary amine nitrogen (N13-C4). These C-N bonds are essentially in the same plane with the plane of benzene and cyclopentene ring. The frontier orbital for all titled complex is plotted in Figure S2. The LUMO surface mostly delocalized within the non-metallic atoms, and for the HOMO level, the Sn atom is overlapped. HOMO which can be thought the outermost orbital containing electrons tends to give these electrons such as an electron donor. LUMO can be thought the innermost orbital containing free places to acceptor electron, owing to the interaction between HOMO and LUMO orbitals, transition of $\pi \rightarrow \pi^*$ type was observed with regard to the molecular orbital theory. As shown in Figure S2 the HOMO is localized over the azomethine group and cyclopentene ring, while the LUMO is localized over the benzene ring and N13-C4 bond. The energy difference between HOMO and LUMO orbitals so called as energy gap is an important stability for structures [36, 37].

The HOMO-LUMO energy gap of the Sn(IV) complexes are shown in Table 7 and revealed that the energy gap reflect to the chemical activity of the complexes. A large HOMO-LUMO gap increases stability and decreases chemical reactivity. The results show the following trend in HOMO-LUMO gap for the complexes:



The $[\text{Me}_2\text{SnCl}_2.\text{H}_2\text{L}^2]$ complex has a large gap between all complexes. A large HOMO-LUMO gap indicate explain the experimental formation constant values. So, the DFT calculations support the experimental formation constant. Absolute hardness is half of the HOMO-LUMO gap. According to the maximum hardness principle, greater hardness (η) causes more stability in the molecule [38]. On the basis of the data in Table 7 $[\text{Me}_2\text{SnCl}_2.\text{H}_2\text{L}^2]$ complex have a higher hardness and is stable than the other complexes.

In order to obtain reliable and stable structures, vibration frequencies were calculated for all optimized complexes. Selected experimental and calculated FTIR vibration frequencies (cm^{-1}) of the complexes were listed in Table 2. The calculated C=C stretching frequency is somewhat different from the experimental data, may be due to the fact that the theoretical data calculated in gas phase. In $[\text{Me}_2\text{SnCl}_2.\text{H}_2\text{L}^2]$ predict stretching modes at 1750, 1560 and 1477 cm^{-1} correspond to C=C bond. C=C bond near the 5-OMe group vibrates at a higher frequency compared to the vibration of C=C bond on the ring in the farthest position to 5-OMe. The C=C stretching mode in cyclopentene rings is 1477 cm^{-1} which occurs at a lower frequency relative to the C=C bond in the ring involving substituent. On the other hand, in $[\text{Me}_2\text{SnCl}_2.\text{H}_2\text{L}^5]$ complexes C=C bond near the 5-NO₂ group vibrates at a lower frequency (1470 cm^{-1}) compared to the vibration of C=C bond on the ring in the farthest position to 5-NO₂ (1490 cm^{-1}) and the C=C stretching mode in cyclopentene rings is appeared at 1474 cm^{-1} . For C-O, C=N and Sn-O stretching frequency showed the agreement between the experimental and scale calculated frequencies.

Base on the optimized structure of the title compound at B3LYP/LANL2DZ level of theory, the atomic charge distributions for all atoms were calculated and the results are listed in Table 8.

Seen from this data, atomic electronegativity plays important roles for atomic charge distributions of the non-hydrogen atoms. Namely, between the two connecting atoms, the atom having bigger electronegativity will carry negative charges, while the atom having smaller electronegativity will carry positive charges. For example, when a carbon atom is connected with a nitrogen atom, the carbon atomic charges are positive values and the nitrogen atomic charges are negative values, since the nitrogen atom has bigger electronegativity than the carbon atom. However, when a nitrogen atom is joined with an oxygen atom, the nitrogen atom has positive charges and the oxygen atom has negative charges, since the oxygen atom has bigger electronegativity than the nitrogen atom. So, for the $[\text{Me}_2\text{SnCl}_2\cdot\text{H}_2\text{L}^5]$ complexes (Table 8), the carbon atoms in cyclopentene and phenyl rings all carry negative charges, since the hydrogen atom has smaller electronegativity than the carbon atom, but C4, C21, C31, C33 and C36 have positive atomic charges. These carbon atoms were joined to nitrogen (imine and nitro group) and oxygen (phenolic group) atoms that have bigger electronegativity than the carbon atom. The N13 and N24 have negatively atomic charges but N54 carry positive charge, because N54 was joined to two oxygen atoms that have electronegativity than the nitrogen atom. On the other hand, for the non-hydrogen atom in Table 8, although atoms of N13, N22, N54 and the carbon atoms in phenyl and cyclopentene rings have negative charge values, steric effect hinders them to coordinate with Sn(IV) ions further. The phenolic oxygen of the ligand has most negative atomic charges, respectively and there is none steric effect hindered, so the phenolic oxygen donates more electron density to the tin atom which has highest positive atomic charge, leading to rather strong Sn-O bonding. This idea is supported by the IR data.

Table 7. The calculated properties for Sn(IV) complexes at B3LYP/Lan2DZ level of theory.

Complexes	HF energies	HOMO/eV	LUMO/eV	gap/eV	Hardness	Dipole/ Debye
$[\text{Me}_2\text{SnCl}_2\cdot\text{H}_2\text{L}^1]$	-979.0946	-0.2125	-0.1168	0.09568	0.04784	9.85
$[\text{Me}_2\text{SnCl}_2\cdot\text{H}_2\text{L}^2]$	-1093.5994	-0.2127	-0.1164	0.09638	0.04892	9.76
$[\text{Me}_2\text{SnCl}_2\cdot\text{H}_2\text{L}^3]$	-993.4285	-0.2151	-0.1262	0.08884	0.04473	7.76
$[\text{Me}_2\text{SnCl}_2\cdot\text{H}_2\text{L}^4]$	-991.6471	-0.2146	-0.1251	0.08947	0.04442	8.05
$[\text{Me}_2\text{SnCl}_2\cdot\text{H}_2\text{L}^5]$	-1183.5643	-0.2188	-0.1372	0.08159	0.04079	5.98

Table 8. The computed Mulliken atomic charges (q/e) of the Sn(IV) complexes.

Atom No.	Charge of $[\text{Me}_2\text{SnCl}_2\cdot\text{H}_2\text{L}^1]$	Atom No.	Charge of $[\text{Me}_2\text{SnCl}_2\cdot\text{H}_2\text{L}^2]$	Atom No.	Charge of $[\text{Me}_2\text{SnCl}_2\cdot\text{H}_2\text{L}^3]$	Atom No.	Charge of $[\text{Me}_2\text{SnCl}_2\cdot\text{H}_2\text{L}^4]$	Atom No.	Charge of $[\text{Me}_2\text{SnCl}_2\cdot\text{H}_2\text{L}^5]$
C1	-0.39089	C1	-0.39088	C1	-0.39085	C1	-0.39091	C1	-0.39064
C2	-0.43132	C2	-0.43135	C2	-0.43139	C2	-0.43130	C2	-0.43152
C3	-0.17114	C3	-0.17162	C3	-0.17043	C3	-0.17093	C3	-0.16879
C4	0.31989	C4	0.32095	C4	0.31970	C4	0.32021	C4	0.31859
C5	-0.45651	C5	-0.45634	C5	-0.45628	C5	-0.45677	C5	-0.45656
C6	-0.29576	C6	-0.29485	C6	-0.29539	C6	-0.29526	C6	-0.29584
S7	-0.17835	S7	-0.17922	S7	-0.17737	S7	-0.17824	S7	-0.17574
S8	0.24048	S8	0.23833	S8	0.24118	S8	0.24078	S8	0.24481
C9	-0.73283	C9	-0.73295	C9	-0.73274	C9	-0.73280	C9	-0.73262
H10	0.23828	H10	0.23815	H10	0.23867	H10	0.23859	H10	0.23922
H11	0.24430	H11	0.24420	H11	0.24441	H11	0.24455	H11	0.24459
H12	0.24455	H12	0.24450	H12	0.24462	H12	0.24443	H12	0.24473
N13	-0.63432	N13	-0.63324	N13	-0.63470	N13	-0.63469	N13	-0.63649
H14	0.21479	H14	0.21486	H14	0.21498	H14	0.21483	H14	0.21533
H15	0.22193	H15	0.22209	H15	0.22262	H15	0.22256	H15	0.22365
H16	0.22317	H16	0.22312	H16	0.22366	H16	0.22360	H16	0.22424
H17	0.23268	H17	0.23274	H17	0.23313	H17	0.23297	H17	0.23353

H18	0.23485	H18	0.23497	H18	0.23522	H18	0.23528	H18	0.23574
H19	0.21385	H19	0.21361	H19	0.21233	H19	0.21333	H19	0.21225
H20	0.42768	H20	0.42835	H20	0.42814	H20	0.42785	H20	0.42760
C21	0.00832	C21	0.00840	C21	0.00852	C21	0.00906	C21	0.00871
C22	-0.21861	C22	-0.21927	C22	-0.21951	C22	-0.21907	C22	-0.22009
C23	-0.65050	C23	-0.65023	C23	-0.65009	C23	-0.65003	C23	-0.65036
N24	-0.52220	N24	-0.51875	N24	-0.51493	N24	-0.51578	N24	-0.50685
H25	0.20859	H25	0.20876	H25	0.20879	H25	0.20957	H25	0.20975
H26	0.21670	H26	0.21735	H26	0.21848	H26	0.21838	H26	0.22074
H27	0.25905	H27	0.26068	H27	0.26092	H27	0.26040	H27	0.26171
H28	0.23191	H28	0.23208	H28	0.23145	H28	0.23088	H28	0.22933
H29	0.23666	H29	0.23697	H29	0.23685	H29	0.23693	H29	0.23749
H30	0.23095	H30	0.23077	H30	0.23191	H30	0.23165	H30	0.23378
C31	0.19811	C31	0.20050	C31	0.19888	C31	0.19963	C31	0.20384
C32	-0.17752	C32	-0.16343	C32	-0.16423	C32	-0.16523	C32	-0.17003
C33	0.43794	C33	0.41541	C33	0.43415	C33	0.43556	C33	0.45503
C34	-0.25877	C34	-0.23836	C34	-0.24049	C34	-0.24224	C34	-0.24620
C35	-0.15174	C35	-0.23286	C35	-0.17078	C35	-0.16705	C35	-0.14433
C36	-0.23880	C36	0.30636	C36	-0.02224	C36	-0.13559	C36	0.05368
C37	-0.16987	C37	-0.20360	C37	-0.18880	C37	-0.18476	C37	-0.14223
O38	-0.89355	O38	-0.91182	O38	-0.89643	O38	-0.89614	O38	-0.87587
H39	0.20791	H39	0.21037	H39	0.21102	H39	0.21112	H39	0.21538
H40	0.21822	H40	0.23111	H40	0.23616	H40	0.23423	H40	0.25461
Sn41	2.11270	Sn41	2.11881	Sn41	2.11314	Sn41	2.11245	Sn41	2.10597
Cl42	-0.67568	Cl42	-0.68109	Cl42	-0.67684	Cl42	-0.67636	Cl42	-0.67159
Cl43	-0.63161	Cl43	-0.63758	Cl43	-0.63248	Cl43	-0.63335	Cl43	-0.62693
C44	-1.21620	C44	-1.21678	C44	-1.21547	C44	-1.21531	C44	-1.21391
C45	-1.21656	C45	-1.21704	C45	-1.21588	C45	-1.21630	C45	-1.21432
H46	0.25331	H46	0.25304	H46	0.25436	H46	0.25422	H46	0.25583
H47	0.25015	H47	0.24824	H47	0.24915	H47	0.24925	H47	0.25005
H48	0.25488	H48	0.25476	H48	0.25568	H48	0.25578	H48	0.25681
H49	0.25359	H49	0.25328	H49	0.25456	H49	0.25468	H49	0.25603
H50	0.25424	H50	0.25409	H50	0.25501	H50	0.25415	H50	0.25609
H51	0.24934	H51	0.24767	H51	0.24850	H51	0.24869	H51	0.24940
H52	0.46656	H52	0.47034	H52	0.46844	H52	0.46861	H52	0.46681
H53	0.25507	H53	0.25804	H53	0.26224	H53	0.26195	H53	0.26449
H54	0.23104	O54	-0.57159	Cl54	-0.04965	Br54	0.06355	N54	0.44261
H55	0.22103	C55	-0.26197	H55	0.25010	H55	0.24837	H55	0.26566
		H56	0.22222					O56	-0.36307
		H57	0.19393					O57	-0.38411
		H58	0.19356						
		H59	0.23222						

In this study, we have synthesized and characterized five new tin(IV) complexes. Physico-chemical measurements confirm the 1:1 Sn(IV) to ligand stoichiometry of the complexes. Thermodynamic properties of the prepared complexes have been investigated. The formation constant of the Schiff bases with dimethyltin(IV)dichloride in DMF decreases according to the following trend $[H_2L^2] > [H_2L^1] > [H_2L^3] > [H_2L^4] > [H_2L^5]$. Biological activity of the ligands and their complexes against different bacteria revealed that the complexes have higher antibacterial activity as compared to the free ligands. We have used density functional theory (DFT) to compute the electronic and molecular structures. The calculated structural parameters for complexes are in good agreement with the experimental data, confirming the obtained geometries for them. The FTIR spectra of the complexes were recorded and the important bands were identified and compared. They can be used for analysis of complexes, help to explain the

behavior of their vibrational modes. The HOMO-LUMO energy gap of the Sn(IV) complexes was calculated. The energy gap reflects to the chemical activity of the complexes. A large HOMO-LUMO gap increases stability and decreases chemical reactivity. The results show the following trend in HOMO-LUMO gap for the complexes: $[Me_2SnCl_2.H_2L^2] > [Me_2SnCl_2.H_2L^1] > [Me_2SnCl_2.H_2L^3] > [Me_2SnCl_2.H_2L^4] > [Me_2SnCl_2.H_2L^5]$.

ACKNOWLEDGEMENTS

We are grateful to Islamic Azad University, Darab branch Council for their financial support. The authors express their sincere thanks to Dr. Banafsheh Esmailzade (Department of Anatomy, Bushehr University of Medical Sciences, Bushehr, Iran) for providing biological data preparation and to Ghazal Mashhadiagha (Department of Chemistry, Shiraz University, Shiraz, Iran) for providing the part of the computational method data.

REFERENCES

1. Lima, V.S.; Lemos, S.S.; Casagrande, G.A. Tributyltin(IV) complexes with amino acid-derived Schiff bases: X-ray and solution structures. *Polyhedron* **2015**, *89*, 85-90.
2. Devi, J.; Devi, S. Synthesis, characterization and antimicrobial evaluation of Schiff base complexes derived from [2,2-(ethylenedioxy)bis(ethylamine)] and 5-chlorosalicylaldehyde. *Der Pharma. Chem.* **2017**, *9*, 89-92.
3. Blunden, S.J.; Cussack, P.A.; Hill, R. *The Industrial Use of Tin Chemicals*, Royal Society of Chemistry: London; **1985**.
4. Wang, F.; Yin, H.; Cui, J.; Zhang, Y.; Geng, H.; Hong, M. Synthesis, structural characterization, in vitro cytotoxicities, DNA-binding and BSA interaction of diorganotin (IV) complexes derived from hydrazone Schiff base. *J. Organomet. Chem.* **2014**, *759*, 83-91.
5. Ali, N.; Khan, A.; Amir, S.; Amir Khan, N.; Bilal, M.; Synthesis of Schiff bases derived from 2-hydroxy-1-naphthaldehyde and their tin(II) complexes for antimicrobial and antioxidant activities. *Bull. Chem. Soc. Ethiop.* **2017**, *31*, 445-456.
6. Kadirvansivasam, K.; Sivajganesan, S.; Periyathambi, T.; Nandhakumar, V.; Chidhambram, S.; Manimekalai, R. Synthesis and characterization of Schiff base Co^{II} , Ni^{II} and Cu^{II} complexes derived from 2-hydroxy-1-naphthaldehyde and 2-picolyamine. *Mod. Chem. Appl.* **2017**, *5*, 1-6.
7. Elsherbiny, A.S.; El-Ghamry, H.A. Synthesis, characterization, and catalytic activity of new Cu(II) complexes of Schiff base: Effective catalysts for decolorization of Acid Red 37 dye solution. *Int. J. Chem. Kinet.* **2015**, *47*, 162-173.
8. Yilmaz, F.; Karaali, N.; Şaşmaz, S.; Microwave-assisted synthesis of some nitro-benzimidazoles and their salicyl and isatin Schiff base. *Bull. Chem. Soc. Ethiop.* **2017**, *31*, 351-359.
9. Esmailzadeh, Sh.; Shekoohi, Kh.; Sharif-Mohammadi, M.; Mashhadiagha, Gh.; Mohammadi, Kh. Synthesis, characterization, spectral Studies, antibacterial evaluation, thermodynamics and DFT calculations of dimethyltin(IV) dichloride Schiff base. *Acta Chim. Slov.* **2015**, *62*, 805-817.
10. Abu-Khadra, A.S.; Farag, R.S.; Abdel-Hady, A.E.M. Synthesis, characterization and antimicrobial activity of Schiff base (*E*)-*N*-(4-(2-hydroxybenzylideneamino)phenylsulfonyl) acetamide metal complexes. *Am. J. Anal. Chem.* **2016**, *7*, 233-245.
11. Kafi-Ahmadi, L.; Shirmohammadzadeh, L. Synthesis of Co(II) and Cr(III) salicylidene Schiff base complexes derived from thiourea as precursors for nano-sized Co_3O_4 and Cr_2O_3 and their catalytic, antibacterial properties. *J. Nanostruct. Chem.* **2017**, *7*, 179-190.

12. Mohammadikish, M. Four coordinate tin complexes: Synthesis, characterization, thermodynamic and theoretical calculations. *Spectrochim. Acta, Part A: Mol. Biomol. Spectros.* **2014**, 117, 175-180.
13. Batral, N.; Malhotra, N.; Assija, S. Organotin(IV) complexes with ONS donor Schiff base ligand: synthesis, characterization and antimicrobial evaluation. *J. Chem. Pharm. Res.* **2014**, 6, 194-200.
14. Nag, K.; Joardar, D. S. Metal complexes of sulphur-nitrogen chelating Agents. I. 2-aminocyclo-pentene-1-dithiocarboxylic acid complexes of Ni(II), Pd(II) and Pt(II). *Inorg. Chim. Acta* **1975**, 14, 133-141.
15. Bordas, B.; Sohar, P.; Matolcsy, G.; Berencsi, P. Synthesis and antifungal properties of dithiocarboxylic acid derivatives. II. Novel preparation of 2-alkylamino-1-cyclopentene-1-dithiocarboxylic acids and some of their derivatives. *J. Org. Chem.* **1972**, 37, 1727-1730.
16. Asadi, M.; Mohammadi, Kh.; Esmailzadeh, Sh.; Etemadi, B.; Fun, H. K. Some new Schiff base ligands giving a NNOS coordination sphere and their nickel (II) complexes: Synthesis, characterization and complex formation. *Polyhedron* **2009**, 28, 1409-1418.
17. Rahman, A.; Choudhary, M.; Thomsen, W. *Bioassay Techniques for Drug Development*, Harwood Academic: Amsterdam; **2001**.
18. Frisch, M.J.; Trucks, G.W.; Schlegel, H.B.; Scuseria, G.E.; Robb, M.A.; Cheeseman, J.R.; Montgomery, J.A.; Vreven, J.T.; Kudin, K.N.; Burant, J.C.; Millam, J.M.; Iyengar, S.S.; Tomasi, J.; Barone, V.; Mennucci, B.; Cossi, M.; Scalmani, G.; Rega, N.; Petersson, G.A.; Nakatsuji, H.; Hada, M.; Ehara, M.; Toyota, K.; Fukuda, R.; Hasegawa, J.; Ishida, M.; Nakajima, T.; Honda, Y.; Kitao, O.; Nakai, H.; Klene, M.; Li, X.; Knox, J.E.; Hratchian, H. P.; Cross, J.B.; Adamo, C.; Jaramillo, J.; Gomperts, R.; Stratmann, R.E.; Yazyev, O.A., Austin, J.; Cammi, R.; Pomelli, C.; Ochterski, J.W.; Ayala, P.Y.; Morokuma, K.; Voth, G.A.; Salvador, P.; Dannenberg, J.J.; Zakrzewski, V.G.; Dapprich, S.; Daniels, A.D.; Strain, M.C.; Farkas, O.; Malick, D.K.; Rabuck, A.D.; Raghavachari, K.; Foresman, J.B.; Ortiz, J.V.; Cui, Q.; Baboul, A.G.; Clifford, S.; Cioslowski, J.; Stefanov, B.B.; Liu, G.; Liashenko, A.; Piskorz, P.; Komaromi, I.; Martin, R.L.; Fox, D.J.; Keith, T.; Al-Laham, M.A.; Peng, C.Y.; Nanayakkara, A.; Challacombe, M.; Gill, P.M.W.B.; Johnson, W.; Chen, W.; Wong, M.W.; Gonzalez, C.; Pople, J.A. *Gaussian 03, Computer Program for Computational Chemistry*, Gaussian Inc.: Pittsburgh PA, USA; **2003**.
19. Becke, A.D. Density functional thermochemistry. III. The role of exact exchange. *J. Chem. Phys.* **1993**, 98, 5648-5652.
20. Akbar Ali, M.; Abu Bakar, H.J.H.; Mirza, A.H.; Smith, S.J.; Gahan, L.R.; Bernhardt, P.V. Preparation, spectroscopic characterization and X-ray crystal and molecular structures of nickel(II), copper(II) and zinc(II) complexes of the Schiff base formed from isatin and S-methyldithiocarbamate (Hisa-sme). *Polyhedron* **2008**, 27, 71-79.
21. Sedaghat, T.; Menati, S. Synthesis and spectroscopic characterization of new adducts of diorganotin(IV) dichlorides with an asymmetric schiff base ligand. *Inorg. Chem. Commun.* **2004**, 7, 760-762.
22. Sihang, S.; Pareek, S.; Gupta, M.; Varshney, S.; Vareshney, A. Spectral and biological investigation of some new Sn(II) complexes with Schiff bases of amino acids. *World J. Pharm. Pharm. Sci.* **2014**, 3, 2164-2176.
23. Kumar, S.B.; Bhattacharya, S.; Dutta, S.K.; Tiekink, E.R.T.; Chaudhury, M. Mononuclear manganese(III) complexes of a heterodonor (N₂OS) ligand containing thiolate-type sulfur: Synthesis, structure, redox and spectroscopic properties. *J. Chem. Soc. Dalton Trans.* **1995**, 16, 2619-2626.
24. Sakthilatha, D.; Rajvel, R. The template synthesis, spectral and antibacterial investigation of new N₂O₂ donor Schiff base Cu(II), Ni(II), Co(II), Mn(II) and VO(IV) complexes derived from 2-Hydroxy acetophenone with 4-chloro-2,6-diaminopyrimidine. *J. Chem. Pharm. Res.* **2013**, 5, 57-63.

25. Yearwood, B. Reaction of tin(IV) chloride and tributyltin chloride with salben^{(t)Bu} [salben^{(t)Bu} = N,N'-(butylene)bis(3,5-di-tertbutyl)salicylideneimine] and salpen^{(t)Bu} [salpen^{(t)Bu} = N,N'-(propylene)bis(3,5-di-tert-butyl)salicylideneimine] ligands. *Int. J. Modern Chem.* **2014**, 6, 65-73.
26. Khan, R.; Tavman, A.; Gurbuz, D.; Arfan, M.; Cinarli, A.; Synthesis and structural characterization of N-(2-[(2E)-2-(2-hydroxybenzylidene)hydrazinyl]carbonyl)-phenylbenzamide HL) and its Co(II), Fe(III), Cu(II) and Zn(II) complexes. X-ray crystal structure of HL. *Bull. Chem. Soc. Ethiop.* **2018**, 32, 111-124.
27. Sharma, R.K.; Singh, Y.; Rai, A.K. Synthesis and characterization of 5- and 6-coordinated monoorganotin(IV) complexes of 2-aminocyclopentene-1-carbodithioic acid and its N-/S-alkyl derivative having NS and SS donor system. *Phosphorus, Sulfur, Silicon, Rel. Elem.* **2000**, 166, 221-230.
28. Casas, J.S.; Sanchez, A.; Sordo, J.; Lopez, V.; Castellano, E.E.; Schpector, J.Z.; Argulles, M.C.R.; Russo, U. Diorganotin(IV) derivatives of salicylaldehydethiosemicarbazone. The crystal structure of dimethyl- and diphenyl-(salicylaldehydethiosemicarbazonato)tin(IV). *Inorg. Chim. Acta* **1994**, 216, 169-175.
29. Otera, J. ¹¹⁹Sn Chemical Shifts in five- and six-coordinate organotin chelates. *J. Organomet. Chem.* **1981**, 221, 57-61.
30. Pellei, M.; Lobbia, G.G.; Mancini, M.; Spagna, R.; Santini, C. Synthesis and characterization of new organotin(IV) complexes with polyfunctional ligands. *J. Organomet. Chem.* **2006**, 691, 1615-1621.
31. Kianfar, A.H.; Abroshan, I. Spectrophotometric study of complexation between some salen type Schiff bases and dimethyltin(IV) dichloride. *Chem. Sci. Trans.* **2013**, 2, 17-24.
32. Leggett, D.L. *Computational Methods for the Determination of Formation Constant*, Plenum Press: New York; **1985**.
33. Tweedy, B.G. Plant extracts with metal ions as potential antimicrobial agents. *Phytopathology* **1964**, 55, 910-914.
34. Dal, H.; Suzen, Y.; Sahin, E. Synthesis, spectral studies of salicylidine-pyridines: crystal and molecular structure of 2-[(1E)-2-aza-2-(5-methyl(2-pyridyl)ethenyl)]-4-bromobenzen-1-ol. *Spectrochim. Acta Part A: Mol. Biomol. Spectros.* **2007**, 67, 808-814.
35. Valente, E.J.; Eggleston, D.S. Structure of (phenyl)bis(4-hydroxybenzo-2H-pyran-2-one-3-yl)methane. *Acta Cryst. Sec. C* **1989**, 45, 785-789.
36. Lewis, D.F.V.; Ioannides, C.; Parke, D.V. Interaction of a series of nitriles with the alcohol inducible isoform of P450: computer analysis of structure activity relationships. *Xenobiotica* **1994**, 24, 401-408.
37. Esmailzadeh, Sh.; Mashhadiagha, Gh. Formation constants and thermodynamic parameters of bivalent Co, Ni, Cu and Zn complexes with Schiff Base ligand: Experimental and DFT calculations. *Bull. Chem. Soc. Ethiop.* **2018**, 31, 159-170.
38. Zhou, Z.; Parr, R.G. New measures of aromaticity: absolute hardness and relative hardness. *J. Am. Chem. Soc.* **1989**, 111, 7371-7379.